# High Internal Inductance Improved Confinement $H$-Mode Discharges Obtained with an Elongation Ramp Technique in the DIII-D Tokamak

L. L. Lao, J. R. Ferron, T. S. Taylor, K. H. Burrell, V. S. Chan, M. S. Chu, J. C. DeBoo, E. J. Doyle,[a] C. M. Greenfield, R. J. Groebner, R. James,[b] E. A. Lazarus,[c] T. H. Osborne, H. St.John, E. J. Strait, S. J. Thompson, A. D. Turnbull, D. Wroblewski,[b] H. Zohm,[d] and DIII-D Team
*General Atomics, San Diego, California 92186*
(Received 1 February 1993)

High confinement mode ($H$-mode) discharges with peaked toroidal current density profile (high inductance, $l_i$) and improved confinement are obtained in the DIII-D tokamak by dynamically varying the current profile using a rapid elongation ramp technique. The confinement improvement increases with $l_i$ and persists in the presence of edge-localized modes. The plasma toroidal rotation and the corresponding radial electric field component also increase with the peakedness of the current density profile.

PACS numbers: 52.55.Fa, 52.25.Fi, 52.25.Vy

The study of plasma energy confinement and methods to improve it has been a very active area of tokamak research [1-7], particularly since the discovery of the high confinement mode ($H$ mode) in the ASDEX tokamak [1]. Before this discovery, tokamak discharges were typically operated in the low confinement mode ($L$ mode) which had a lower energy confinement than $H$-mode discharges. An improved tokamak energy confinement, together with the ability to operate at high plasma energy density (high plasma beta) and advances in the area of heat flux handling capability of the plasma facing components in the first wall of a tokamak, can potentially lead to a more compact and economically more attractive fusion reactor. In this Letter, we report recent experimental results from the DIII-D tokamak which show that plasma energy confinement in $H$-mode discharges can be further improved by varying the shape of the current profile. The results suggest that detailed current profile control may lead to better prospects for a fusion reactor based on the tokamak concept.

This experimental study is motivated by the recent confinement results from current ramp experiments in $L$-mode limiter plasmas from various tokamaks [5-7], where it has been observed that the plasma energy confinement improves with the peakedness of the current profile shape in addition to the usual dependence on the plasma current $I_P$. The energy confinement time $\tau_E$ is found to scale as the product of the plasma internal inductance, $l_i \equiv \int dV B_P^2/[V\bar{B}_P^2(1)]$, which is a measure of the peakedness of the current profile, and $I_P$, $\tau_E \propto l_i I_P$. Here, $B_P$ is the poloidal magnetic field, $V$ is the plasma volume, $\bar{B}_P(x) \equiv \oint_x dl B_P/\oint_x dl$ is the average poloidal magnetic field on a flux surface, and $0 \le x \equiv [V/V(1)]^{1/2} \le 1$ is a flux surface label. Because of the potential usefulness of $H$-mode plasmas in advanced fusion reactor applications, it is important to investigate whether this method of confinement improvement by current profile control can be applied to $H$-mode plasmas. The present experiments are designed to further test the effects of the current profile on the energy confinement in highly shaped divertor $H$-mode plasmas by making use of the unique shaping capability of the DIII-D tokamak. Unlike the current ramp method, which simultaneously varies both the shape of the current profile $l_i$ and $I_P$, this new technique is capable of varying only the current profile shape while keeping $I_P$ constant. Thus, the experiments can yield additional important physical insight into the energy transport mechanisms.

In these experiments, $H$-mode discharges with energy confinement enhancement factor up to 1.8 times the $H$-mode values [8] and 3 times the $L$-mode values [9] are obtained. These high confinement discharges are produced by dynamically increasing the elongation $\kappa$ of the plasma poloidal cross section at a fast rate, $\dot{\kappa} > 2$/s, after initiation of the beam heating phase. Both the neutral beam injection power $P_{\rm NBI}$ and $I_P$ are held fixed during the $\kappa$ ramp. Since the current diffusion time in the hot plasma center is long relative to that in the edge region, the current channel is trapped in the plasma core, producing a very peaked current density profile. Values of $l_i$ greater than 1.8 have been obtained. The $\kappa$ ramp serves both to create a peaked current density profile and to induce an $L$-mode to $H$-mode transition. When the maximum $\kappa$ exceeds 1.8, $H$-mode discharges are obtained. The energy confinement improves with $l_i$ and then slowly decreases to the standard $H$-mode value as the current profile relaxes and edge-localized modes (ELMs) occur. ELM is an edge-localized relaxation which reduces the edge plasma pressure gradient by enhancing the particle and energy transport [10]. In these discharges, the confinement improvement persists in the presence of ELMs.

The temporal evolution of a $\kappa$ ramp discharge is given in Fig. 1. Starting from a low $\kappa \sim 1.3$, inside limiter plasma (Fig. 1), $\kappa$ is increased to $> 1.8$ in 200 ms with $I_P$ and $P_{\rm NBI}$ held fixed at 1.0 MA and 5.7 MW. Around 2120 ms, when $l_i \sim 1.8$ and $\kappa \sim 1.8$, the plasma makes a transition into the $H$-mode phase. Note that here the $L$-$H$ transition is induced by the change in $\kappa$. After the $L$-$H$ transition, the discharge remains ELM-free for about

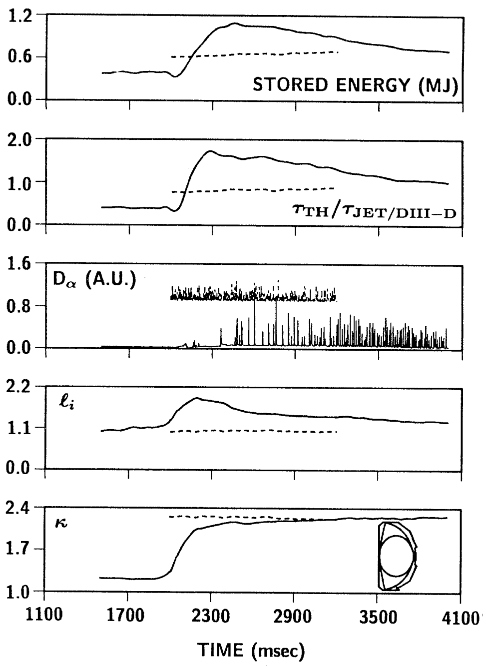


FIG. 1. Time evolution of $W_T$, $\tau_N$, the line-averaged $n_e$, divertor $D_\alpha$ radiation, $l_i$, and $\kappa$ for a $\kappa$ ramp discharge with $P_{\rm NBI}=5.7$ MW (solid traces) and a constant $\kappa$ reference $H$-mode discharge with $P_{\rm NBI}=6.2$ MW (dotted traces). Also shown in the bottom panel are the poloidal cross sections from equilibrium analysis for the $\kappa$ ramp discharge at 1950 ms and 2350 ms.

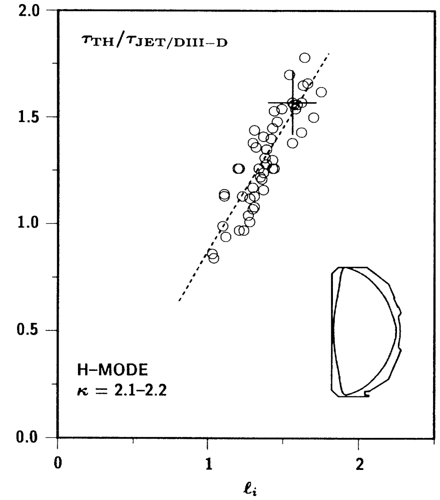


FIG. 2. Variation of the normalized thermal energy confinement time with $l_i$, $I_P=1-1.5$ MA, $P_{\rm NBI}=4-12$ MW, $\tau_{\rm JET/DIII\text{-}D}(\rm s)\equiv 0.106 P_L^{-0.46}(\rm MW) I_P^{1.03}(\rm MA) R^{1.48}(\rm m)$ [8]. Also shown is the plasma poloidal cross section.

240 ms and then ELM starts. Despite the presence of ELMs, the thermal energy confinement times, $\tau_{\rm TH} \equiv W_{\rm TH}/P_L$, remains substantially higher than values expected using the JET/DIII-D ELM-free $H$-mode scaling [8], $\tau_{\rm JET/DIII\text{-}D}$. Here, $W_{\rm TH}$ is the plasma thermal energy, $P_L \equiv P_T - \dot{W}_T$ is the plasma loss power, $W_T$ is the plasma stored energy, and $P_T$ is the total heating power. The variation of $\tau_N \equiv \tau_{\rm TH}/\tau_{\rm JET/DIII\text{-}D}$ during the slow current relaxation phase correlates well with the change in $l_i$. Note that in current ramp experiments in $L$-mode plasmas [5–7], $W_T$ and $\tau_E$ are observed to decay slowly and only $\tau_E/I_P$ is observed to increase. Here, in addition to $\tau_E/I_P$, the magnitude of both $W_T$ and $\tau_E$ are found to improve following the change in the current profile shape. In Fig. 1, the values of $W_T$ and $l_i$ are obtained from the external magnetic measurements using equilibrium analysis [11]. $W_{\rm TH}$ and $\tau_{\rm TH}$ are determined from $W_T$ by subtracting the fast ion stored energy calculated approximately using an analytical formula. For the time slices when the density and the temperature profile measurements are available, these approximate values of $W_{\rm TH}$ and $\tau_{\rm TH}$ agree within $\sim 10\%$ with the values obtained from the full kinetic profile measurements.

The effects of the $\kappa$ ramp on the discharge can be seen more clearly by comparing to a reference constant $\kappa$ ELM $H$-mode discharge, also shown in Fig. 1. The reference discharge has $\kappa \sim 2.2$, $l_i \sim 1.0$, and $\tau_N \sim 0.9$. It has a double-null divertor shape similar to that obtained in the later part of the $\kappa$ ramp discharge. Comparison of the confinement results from these two discharges suggests that the observed confinement improvement during the current relaxation phase in the $\kappa$ ramp discharge is due mainly to change in the toroidal current density profile.

The data obtained from several $\kappa$ ramp experiments, taken during the ELM and low current relaxation phase of these discharges, when $\dot{W}_T/P_T \lesssim 0.15$ with $I_P=1-1.5$ MA and $P_{\rm NBI}=4-12$ MW, are summarized in Fig. 2. Most of the data are for $I_P=1$ MA at moderate beam power. $\tau_N$ is observed to vary approximately linearly with $l_i$. These results are similar to those obtained in current ramp experiments in $L$-mode plasmas in various tokamaks [5–7].

The global observation of confinement improvement with $l_i$ can also be seen in the increase of electron and ion temperatures and electron density ($T_e$, $T_i$, and $n_e$) with the peakedness of the current density profile. This is illustrated in Figs. 3(a)–3(c), where profiles of $T_e$, $T_i$, and $n_e$ for the $\kappa$ ramp discharge shown in Fig. 1 at various times are compared. These profiles of $T_e$, $T_i$, and $n_e$ are obtained from the Thomson scattering and the horizontal electron cyclotron emission diagnostics, the charge exchange recombination (CER) diagnostic, and the Thomson scattering and the interferometry diagnostics, respectively. Note that 3200 ms, $T_e$ in the edge region has nearly approached a stationary value while $T_e$ in the central region and $n_e$ are still relaxing.

Various theoretical and empirical models based on the electron response in a stochastic magnetic field due to magnetic turbulence [12], neoclassical bootstrap current

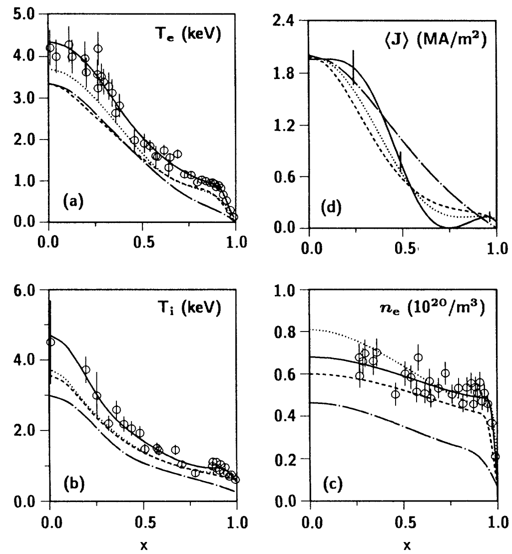


FIG. 3. (a)-(d) Comparison of $T_e$, $T_i$, $n_e$, and $\langle J \rangle$ at the $L$-mode time 1950 ms (chain-dotted curves), $l_i \sim 1.1$; and at the $H$-mode times 2500 ms (open circles and solid curves), $l_i \sim 1.7$; 3200 ms (dotted curves), $l_i \sim 1.4$; and 4000 ms (dashed curves), $l_i \sim 1.2$ for a $\kappa$ ramp discharge.

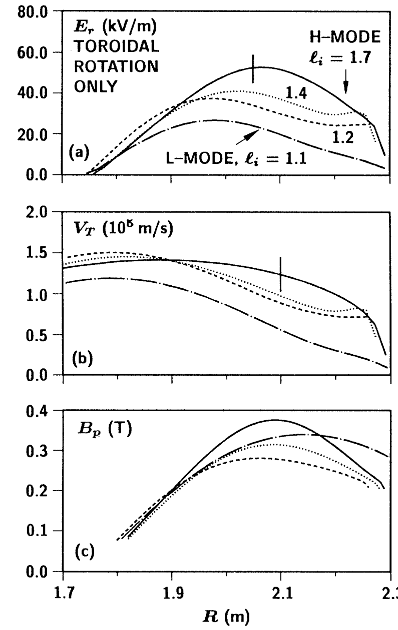


FIG. 4. (a)-(c) Comparison of $V_T$, $B_P$, and $E_R$ due to $V_T$ across the midplane at 1950 ms (chain-dotted curves), 2500 ms (solid curves), 3200 ms (dotted curves), and 4000 ms (dashed curves) for a $\kappa$ ramp discharge.

driven turbulence [13], and anomalous electron viscosity [14] have been proposed, which suggest that plasma energy confinement improves with the magnetic shear, $S_B \equiv xq'(x)/q$ and the poloidal magnetic field $B_P$. A peaked current density profile increases $S_B$ in the plasma outer region and $B_P$ in the plasma interior region. In Fig. 3(d), profiles of the flux surface average toroidal current density $\langle J \rangle$ at various times are compared. These $\langle J \rangle$ profiles are reconstructed from equilibrium analysis [11] using the measured kinetic profiles, the external magnetic measurements, and a single channel motional Stark effect (MSE) measurement. Equilibrium reconstruction using the newly installed eight-channel MSE diagnostic [15] and magnetic data for a recent similar discharge show similar profiles. Profiles of $B_P$ across the plasma midplane associated with these current density profiles are shown in Fig. 4(c). Transport simulations using neoclassical resistivity and a simple sawtooth relaxation model with the measured density and temperature profiles as inputs show qualitatively similar current density profiles but with a larger edge current density, particularly during the ELM relaxation phase. The calculated bootstrap current fraction in this discharge is 20%-30%.

Sheared flow stabilization of turbulence due to the radial electric field shear has been shown to be a leading candidate responsible for the confinement improvement in $H$-mode discharges [16], and more recently for the enhanced confinement in $VH$-mode discharges [4]. In these new experiments, the plasma toroidal rotation velocity $V_T$ is also found to increase with the peakedness of the toroidal current density profile. This is illustrated in Fig. 4(b), where profiles of $V_T$ across the plasma midplane obtained from the CER diagnostic at various times are compared. As is shown, $V_T$ in the edge region, $R \sim 2.2$ m, increases by nearly a factor of 2.5 from before to after the $\kappa$ ramp. $V_T$ then decreases as the current profile relaxes. The increases in $V_T$ and internal $B_P$ give rise to an increase in the radial electric field ($E_R$) component due to this rotation motion, $V_T B_P$, and its shear, $S_E \equiv \partial E_R / \partial R$. This is illustrated in Fig. 4(a), where profiles of $E_R$

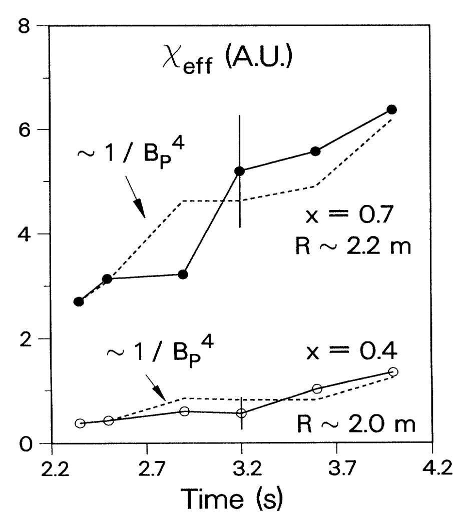


FIG. 5. Comparison of $\chi_{eff}$ at $x = 0.4$ and 0.7.

across the midplane due to $V_T$ at various times are compared. In the plasma interior region, $x < 0.8$, the $V_T$ component is the dominant contributor to $E_R$. Both $E_R$ and $S_E$ increase with $B_P$ and decrease as the current profile relaxes and $B_P$ decreases.

Consistent with the observation of global energy confinement improvement with $l_i$, the local single fluid thermal diffusivity $\chi_{\text{eff}}$ decreases with increasing $B_P$. This is illustrated in Fig. 5, where values of $\chi_{\text{eff}}$ at $x = 0.4$ and 0.7 at various times are compared. $\chi_{\text{eff}}$ is obtained from time-dependent transport analysis using the measured density and temperature profiles. As is shown, $\chi_{\text{eff}}$ increases by nearly a factor of 2–3 as the current density profile relaxes. This increase in $\chi_{\text{eff}}$ is representative of the plasma in the region $0.3 < x < 0.8$, where the confinement is little affected by sawtooth and ELM relaxation. In this region, $\chi_{\text{eff}}$ varies approximately at $1/\bar{B}_P^{\alpha}$ as the current profile relaxes, where $\alpha \sim 3$–4. This dependence of $\chi_{\text{eff}}$ on $\bar{B}_P$ is stronger than that observed in current ramp experiments where $\alpha \sim 1$–2 [6,7]. The dependence of $\chi_{\text{eff}}$ on $S_B$ appears to be weaker. All of the models [12–14] discussed previously exhibit qualitatively this local $\bar{B}_P$ dependence of $\chi_{\text{eff}}$.

As has been shown, a peaked current density profile increases $B_P$ in the plasma interior region, $S_B$ in the plasma outer region, and $E_R$ and $S_E$ in much of the plasma interior region. All of these may contribute to the observed improvement confinement in these high $l_i$ $\kappa$ ramp discharges. In the $\kappa$ ramp experiments, since $E_R$ and $S_E$ also increase with $B_P$, the effects of $S_E$ on transport can also appear as a $B_P$ dependence. However, in the region $R \sim 2.05$ m where $S_E$ is weak, improvement of $\chi_{\text{eff}}$ is still observed, which suggests other mechanisms also play a role in the confinement improvement. Further experiments and studies are needed to separate the roles of $B_P$, $S_B$, and $S_E$ in the confinement improvement observed in these high $l_i$ $\kappa$ ramp discharges.

The results from these experiments indicate that high energy confinement is obtainable with a peaked current density profile (high $l_i$), sufficient degree of shaping, and perhaps some requirement for edge current density. These results suggest that, with detailed current and heating profile control in shaped tokamak discharges, steady state and high performance tokamak operation may be possible.

This work was supported by the U.S. Department of Energy under Contract No. DE-AC03-89ER51114.

[a]Permanent address: University of California, Los Angeles, CA 90024.

[b]Permanent address: Lawrence Livermore National Laboratory, Livermore, CA 94551.

[c]Permanent address: Oak Ridge National Laboratory, Oak Ridge, TN 37831.

[d]Permanent address: Max-Planck-Institut für Plasmaphysik, Germany.

[1] F. Wagner *et al.*, Phys. Rev. Lett. **53**, 1453 (1984).

[2] J. D. Strachan *et al.*, Phys. Rev. Lett. **58**, 1004 (1987).

[3] B. J. D. Tubbing *et al.*, Nucl. Fusion **31**, 839 (1991).

[4] G. L. Jackson *et al.*, Phys. Rev. Lett. **67**, 3098 (1991).

[5] M. C. Zarnstorff *et al.*, in *Plasma Physics and Controlled Nuclear Fusion Research, 1990* (International Atomic Energy Agency, Vienna, 1991), Vol. 1, p. 109.

[6] C. D. Challis *et al.*, Nucl. Fusion **32**, 2217 (1992).

[7] J. R. Ferron *et al.* (to be published).

[8] D. P. Schissel *et al.*, Nucl. Fusion **31**, 73 (1991).

[9] P. N. Yushmanov *et al.*, Nucl. Fusion **30**, 1999 (1990).

[10] P. Gohil *et al.*, Phys. Rev. Lett. **61**, 1603 (1988).

[11] L. L. Lao *et al.*, Nucl. Fusion **30**, 1035 (1990).

[12] P.-H. Rebut *et al.*, Phys. Fluids B **3**, 2209 (1991).

[13] O. J. Kwon *et al.*, Phys. Fluids B **2**, 291 (1990).

[14] K. Itoh *et al.*, in "Plasma Physics and Controlled Nuclear Fusion Research, 1992" (International Atomic Energy Agency, Vienna, to be published).

[15] D. Wroblewski *et al.*, Rev. Sci. Instrum. **63**, 5140 (1992).

[16] K. H. Burrell *et al.*, Plasma Phys. Controlled Fusion **34**, 1859 (1992).